An Investigation of the Conformation of β-Carrageenan by Molecular Mechanics and Molecular Dynamics Simulations

Kazuyoshi Ueda*, Hiroshi Ochiai, Akira Imamura,† and Setsuko Nakagawa††

Department of Chemistry, Faculty of Science, Hiroshima University, Kagamiyama, Higashi-Hiroshima 724

†Department of Chemistry, Faculty of Science, Hiroshima University, Kagamiyama, Higashi-Hiroshima 724 and Group, PRESTO, Research Development Corporation of Japan, Tsukuba Research Consortium, Tsukuba 300-26

††Institute for Fundamental Chemistry, 34-4 Takano Nishikai-cho, Sakyo-ku, Kyoto 606

(Received April 1, 1994)

Carrageenan is known to change its conformation from coil to helix and to form a gel. However, the accurate conformation and the transition mechanism have not yet been detailed. In this work, the conformational behavior of β-carrageenan (a copolymer with a carrabiose repeating unit, 1,4-linked 3,6-anhydro-α-D-galactose (**A**) and 1,3-linked β-D-galactose (**B**)), was studied by using molecular mechanics and molecular dynamics simulation methods with the program CHARMM22. The energy maps of the carrabiose as a function of the dihedral angles of the glycosidic linkages between the **A**–**B** (1–3 linkage) and **B**–**A** (1–4 linkage) carrabiose units were calculated. Both carrabiose units were found to have five deep potential energy minima. Based on these carrabiose conformations, 25 conformers of the single helical chain carradodecaose were constructed and their minimum energy conformations were investigated by molecular mechanics and molecular dynamics simulations. From the results of these analyses, a possible single helical structure of β-carrageenan was elucidated. The stability of this helical conformation is discussed by comparing it with a double helical conformation, which was found from X-ray diffraction analyses of oriented fiber samples of κ- and ι-carrageenans, which are well-studied members of the carrageenan family.

The carrageenans are polysaccharides extracted from *red algae*. There are several members in this family whose basic structure is an alternating linear copolymer with repeating carrabiose units of 1,3-linked β-D-galactose (**B**) and 1,4-linked 3,6-anhydro-α-D-galactose (**A**) as shown in Fig. 1. They have been of great interest in both practical and theoretical fields, since they form thermoreversible gels. The basic mechanism of the gelation has been thought to be attributed to the two steps of the conformational transition; the first step is a transition from coil to helix, and the next is an aggregation process of these helices.[1—3] But, the exact mechanism is still controversial. Especially, the structural details of the helix, whether it is single or double, are still unclarified and have been discussed for many years. Anderson et al.[4] proposed a double helix model from X-ray diffraction experiments using oriented fiber samples of κ- and ι-carrageenans. Since then, the molecular conformation of carrageenan has been thought to be the same double helical structure in aqueous systems. On the contrary, Smidsrod and Grasdalen[5] showed the possibility of a single helical form from molecular weight determinations by light scattering and/or thermodynamic experiments. However, the exact model of the molecular conformation for this single helical structure has not been proposed yet. Until now, many reports have been published on this subject.[6—9] But, because of the complicated behavior of the carrageenan solution, the exact conformation and its transition mechanism have still not been detailed.

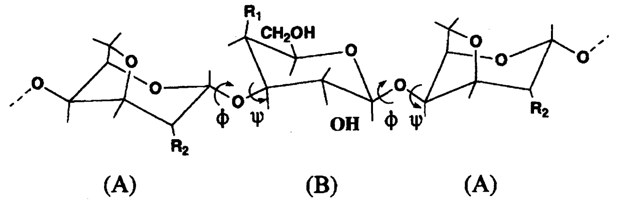

Fig. 1. Structure of carrageenan; ι-carrageenan ($R_1=OSO_3^-$, $R_2=OSO_3^-$), κ-carrageenan, ($R_1=OSO_3^-$, $R_2=OH$), β-carrageenan ($R_1=OH$, $R_2=OH$), Furcellaran ($R_1=OH$ (40%) and OSO_3^- (60%), $R_2=OH$, (A): 3,6-anhydro-α-D-galactose unit, (B): β-D-galactose unit.

In this work, we have attempted to use molecular mechanics and molecular dynamics calculations as a first step to investigate the solution conformation of carrageenan, by using a computer simulation method. Recent progress in the simulation method enables us, in principle, to calculate the fairly large system which

includes solvent water molecules explicitly around the carbohydrate molecule.[10—13] But, actually, such a simulation is still limited to carbohydrates with a molecular size up to an oligomer at present, because the available computers still have limited abilities. Therefore, for the calculation of larger carbohydrate molecules, the effects of solvent molecules should be treated with some approximations. In most cases, such effects have been partly included by changing the dielectric constant as an electrostatic screening effect due to the surrounding medium.[14—16] In this study, we also used this approach to obtain basic information about the conformational state of carrageenan.

The carrageenans are distinguished mainly by the contents of the sulfate group on the carrabiose disaccharide repeating unit. Namely, κ- and ι-types have one and two sulfate groups respectively, as shown in Fig. 1. Furcellaran has about 60% sulfated R_1 and nonsulfated R_2 sites, and the β-type has ideal nonsulfated, that is, uncharged disaccharide units.[17] Generally, the species with lower amounts of sulfate esters are known to have a higher gel-forming ability. Although a β-carrageenan with a completely uncharged molecular structure has not been found as a natural product, knowledge of this uncharged polysaccharide would be useful as basic information for the uncharged state to understand the conformation and the gelling properties of the carrageenan family with different charge densities. Therefore, in this study, an ideal uncharged β-carrageenan was used as the first step to obtain conformational information about the carrageenan family.

The carrabiose units of β-carrageenan were used for the calculation of the energy map of the torsional angles of the glycosidic linkages. Based on the energy minima conformations for these carrabiose units, we first investigated the single helical chain conformation of β-carrageenan of oligomer size. Knowledge of the single chain conformation is important for further consideration of the interchain interactions of carrageenans, such as helical association and/or gel formation. From the molecular mechanics calculations on some helical conformers of carradodecaose, a possible conformation of the single helical structure of β-carrageenan can be elucidated. The stability of this helical structure was examined by molecular dynamics simulations in comparison with the results of the double helical structure with the same dodecamer unit.

Procedures

1. Structure. The atoms of the 3,6-anhydro-α-D-galactose (**A**) and β-D-galactose (**B**) groups are numbered as shown in Fig. 2. In the calculations of the disaccharide units, two types of carrabiose model structures with different glycosidic linkages, 1–4 linked **B–A** and 1–3 linked **A–B**, are used. The sugar residue shown on the left side is always denoted as a nonreduced ring. The glycosidic torsion angles

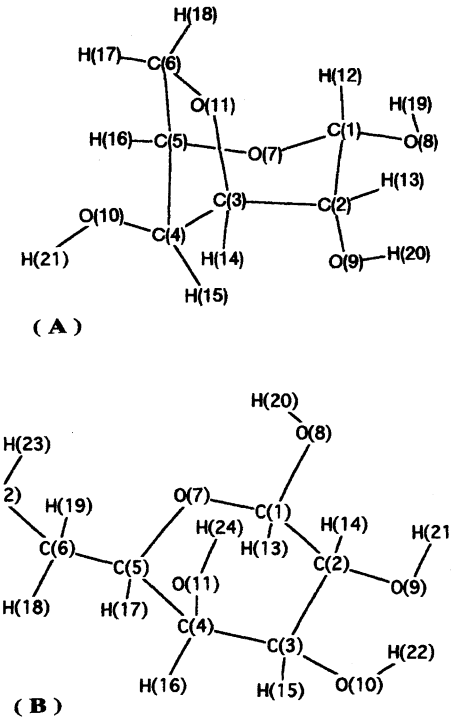

Fig. 2. Structure and the numbering of the atoms of 3, 6-anhydro-α-D-galactose (**A**) and β-D-galactose (**B**).

of ϕ and ψ are defined as ϕ (C2B–C1B–O10A–C4A) and ψ (C1B–O10A–C4A–C3A) for 1–4 linked **B–A** units, and ϕ (C2A–C1A–O10B–C3B) and ψ (C1A–O10B–C3B–C2B) for 1–3 linked **A–B** units, respectively. These angles are always measured from their *cis* positions. For carradodecaose models, the numbering begins from the nonreduced **B** ring to the reduced **A** end, such as B1–A2–B3–···A12.

2. Molecular Mechanics and Molecular Dynamics Calculations. Molecular mechanics and molecular dynamics calculations were carried out by using the CHARMM22 program.[18] The potential energy function is a general form containing terms for bond stretching, angle bending, torsional rotations, and van der Waals and coulombic interactions. The force constants used were those of a CHARMM-type force field proposed for carbohydrates by Ha et al.[19] Long-range interactions were cut off between 10.0 and 12.0 Å by use of a switching function.[18] In the calculation of the electrostatic force, the dielectric constant was set at 3 in order to approximate the electrostatic screening effect by the surrounding medium in vacuo calculation. This value is frequently used in similar calculations, such as those by Hardy and Sarko,[14] Brady,[20] and others.[21,22] For comparison, the results for $\varepsilon=80$ were also calculated for the cases where the solvent screening was strong enough. The partial atomic charges for each atom on the molecule were obtained by ab initio MO calculations with GAUSSIAN 92.[23] These values depend on the basis set used. The magnitude of the atomic charge was too small when the STO-3G basis

set was used. When a larger basis set was used, the obtained values did not show any large dependence on the selection of the basis sets.[24] In this work, the values obtained by using the 6-311G* basis set and with the Merz–Singh–Kollman method[25,26] were used in all calculations. The obtained values for the residues of 3,6-anhydro-α-D-galactose and β-D-galactose are shown in Table 1. The obtained values are in good accordance with those obtained by Ha et al. for the glucose residue.[19]

Energy minimization was achieved by use of a steepest-descent method for the initial minimization and the adopted basis set Newton–Raphson method (ABNR) for final minimization. The molecular dynamics calculations were carried out using a Verlet integrator with a step size of 1 fs and at a constant temperature of 300 K. Hydrogen atoms were kept rigid using the SHAKE constrained algorithm. The molecules were equilibrated for a period of 50 ps in each simulation. Data analysis was performed for the following 500 ps for single chain carradodecaose, and 250 ps for double a helix which consisted of two strands of carradodecaose chains.

Results and Discussion

1. Potential Energy Maps for Carrabiose Units. The main factor in the determination of the conformation of linear polysaccharides, such as β-carrageenan, is the dihedral angles of the glycosidic linkages between the sugar rings. In the structure of β-carrageenan, two kinds of glycosidic linkages exist between **B–A** (1–4 linkage) and **A–B** (1–3 linkage) disaccharide units. Figure 3 shows the potential energy maps of the glycosidic linkages for these carrabiose units. These maps were obtained by allowing the molecular structure to relax to give the lowest energy conformation corresponding to each combination of fixed glycosidic angles, which were selected at 20 °C intervals on a grid in (ϕ, ψ) space. There are five deep low energy minima in the (ϕ,ψ) map of 1–4 linked **B–A**, which were denoted by letters from a to e. The map of the 1–3 linked **A–B** also has five low potential energy minima termed f to j. The positions of these minima and their relative energies are shown in Table 2. It can be seen in Table 2 that the relative energy differences at the minima a, d, and e in the map of the 1–4 linkage, and h and i of the 1–3 linkage, are only around 1 kcal mol^{-1} or less, which is comparable to the energy of thermal fluctuation at room temperature (RT≅0.6 kcal mol^{-1} at 30 °C). This means that each of these disaccharide units can not keep its glycosidic angles in a particular potential well with the lowest energy, but fluctuates among these low energy minima with occupation probability determined by the Boltzmann distribution function. Similar transition behavior is frequently observed in other disaccharide units, such as maltose[10] and cellobiose.[14] However, it should be noted that the polysaccharide, β-carrageenan, which has some carrabiose repeating units in its linear chain, can still take a particular conformation, such as a helical structure, where the conformational energy would be lowered by the additional intermolecular stabilization between spatially accessible residues by long range interactions. Hydrogen bonds and van der Waals forces can act as these stabilization interactions between closely associated residues in such a helical structure. These possibilities were then investigated with a carradodecaose model of β-carrageenan.

Table 1. Partial Atomic Charges Obtained by the ab initio MO Calculation

Atom	β-D-Galactose	Atom	3,6 Anhydro-α-D-galactose
C1	0.44	C1	0.41
C2	0.22	C2	0.44
C3	0.33	C3	−0.15
C4	−0.07	C4	0.46
C5	−0.11	C5	0.04
C6	0.45	C6	0.04
O7	−0.42	O7	−0.49
O8	−0.75	O8	−0.80
O9	−0.77	O9	−0.80
O10	−0.70	O10	−0.81
O11	−0.61	O11	−0.46
O12	−0.74	H12	0.05
H13	0.03	H13	0.01
H14	0.08	H14	0.16
H15	0.01	H15	0.08
H16	0.18	H16	0.12
H17	0.10	H17	0.07
H18	0.03	H18	0.09
H19	−0.02	H19	0.52
H20	0.49	H20	0.52
H21	0.49	H21	0.50
H22	0.46		
H23	0.45		
H24	0.45		

2. Single Chain Helical Conformation. The single chain helical conformation of β-carrageenan was investigated by using some conformers of carradodecaose. In order to construct the initial structures of these

Table 2. The Energy Minimum Points and Their Relative Energies at Various Wells

Linkage	Well	ϕ	ψ	Relative energy
		degree	degree	kcal mol^{-1}
	a	67	173	0.8
	b	177	186	1.3
1—4	c	298	196	1.9
	d	180	295	0.0
	e	305	294	0.2
	f	188	40	4.8
	g	63	179	3.4
1—3	h	175	182	0.0
	i	183	260	1.1
	j	189	279	4.0

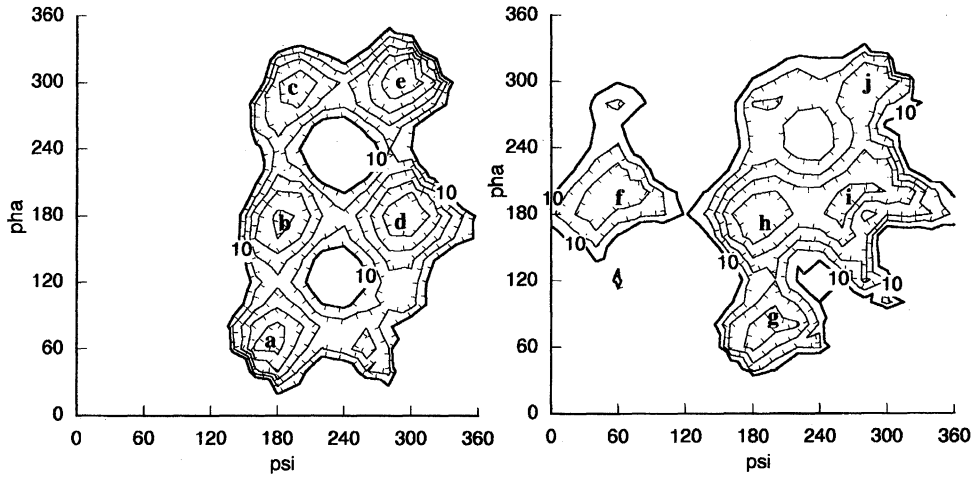

Fig. 3. Contour maps of the potential energy surface in (ϕ,ψ) space for carrabiose unit of 1–4 linked **B–A** (left) and 1–3 linked **A–B** (right). a—j indicate the potential wells. Contour interval is 2 kcal mol^{-1}.

helical conformers, the glycosidic angles of (ϕ, ψ) between the 1–4 linkages of all **B–A** residues in the carradodecaose were set to the same value which was selected from the potential minima from a to e shown in Fig. 3. In a similar manner, the dihedral angles of the glycosidic 1–3 linkages between the residues of all **A** and **B** units were selected from f to j in the same figure. The above combination of dihedral angles produced 5×5 helical conformers, which were denoted by a number from 1 to 25 for the conformers with dihedral pairs of a·f, a·g, a·h,···e·h, e·i, e·j, respectively. Energy minimization was performed on all the above conformers and their energy minimum conformations and potential energies were obtained. The potential energy for each helical conformation after minimization is shown in Fig. 4. The third pair of the dihedral angles, a·h, was found to have the lowest value in this figure. All other conformers have higher energy values are 42 or more kcal mol^{-1} larger than that of the a·h helix. These energy differences correspond to 7 kcal mol^{-1} or more per disaccharide unit, which may be sufficient to prevent the transition from the a·h helix to other conformations. This indicates that the a·h helix exists as a stable conformation. The structure of this helix is schematically shown as a stereo view in Fig. 5(a). It forms a left-handed helical structure with large loops. This loop structure is more clearly shown in Fig. 6 as a projection along the helical axis. The loop consists of 8 sugar residues per turn and has a large cavity at the center. An interesting point is that the size of this loop is quite similar to that of cyclodextrin, especically γ-type cyclodextrin, which also has the same 8 sugar residues in its structure.[27] By analogy with the function of cyclodextrin, the single helical structure of β-carrageenan may have the ability to form a host–guest complex. The similar helical conformation with large loop structure can be seen in some other polysaccharides. Amylose forms a host–guest complex with iodine molecules, whose structure is a single helix with 6—7 sugar residues per turn,[28] although it

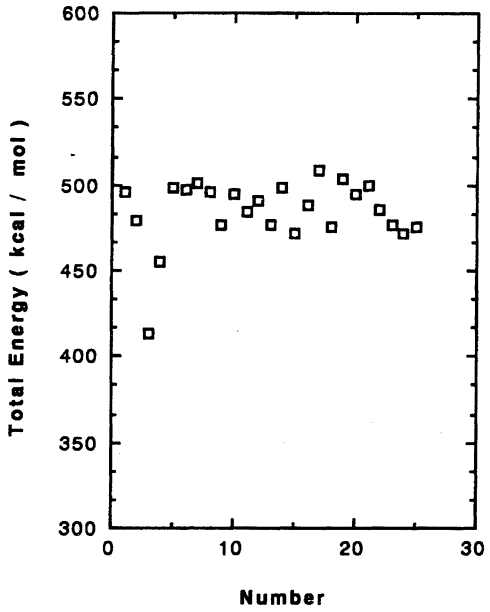

Fig. 4. Total energy of the single helical conformers of carradodecaose β-carrageenan after minimization with ε=3. The abscissa indicates the pair number of the glycosidic dihedral angles. See the detail in the text.

forms a 6/1 double helical conformation in crystalline structure.[29,30] Curdlan also is thought to have a similar helical conformation of a 6/1 single helix and 6/1 triple helix, which depends on the solution conditions.[31,32]

For a more detailed investigation of the helical structure of β-carrageenan, the total energy was divided into individual energy terms. These values are shown in Fig. 7. In the electrostatic interaction term, the conformation of the a·h helix (number 3) takes the lowest value compared to the other conformers. However, number 3 does not take the lowest, but shows rather higher values in other potential terms. This result shows that the a·h single helix may exist as the conformation with the lowest electrostatic potential. This

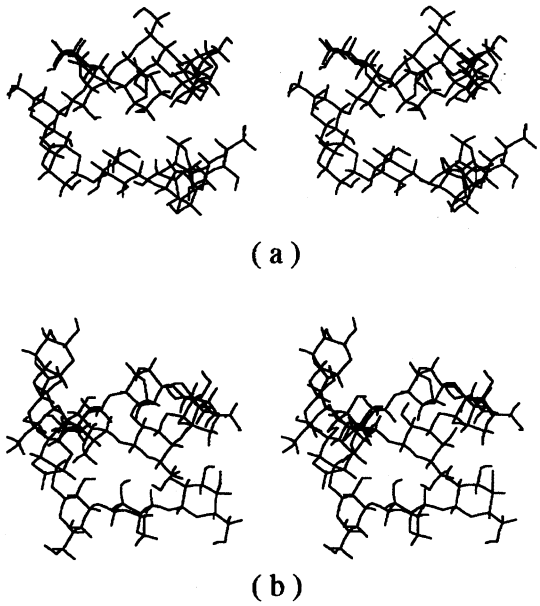

Fig. 5. Stereo views of the initial conformation after minimization and its snap shot at the 550 ps dynamics of the single helical conformation of carradodecaose β-carrageenan with a·h pair dihedrals.

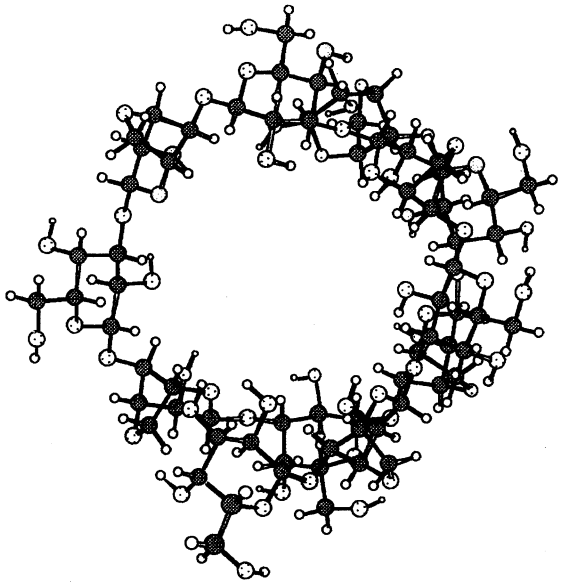

Fig. 6. Schematic figure of the single helical structure of carradodecaose β-carrageenan, which was shown as a projection along to the helical axis.

conformation may include some electrostatic interaction sites such as the formation of hydrogen bonds between some particular sites in this helical conformation. But, these kinds of interaction sites have not yet been identified in this work, as should be studied in the future.

An additional calculation was performed by using $\varepsilon=80$ in order to estimate the limiting case when the electrostatic force was sufficiently shielded by the surrounding water molecules. The results are shown in Fig. 8. Conformation number 3 is still one of the lowest

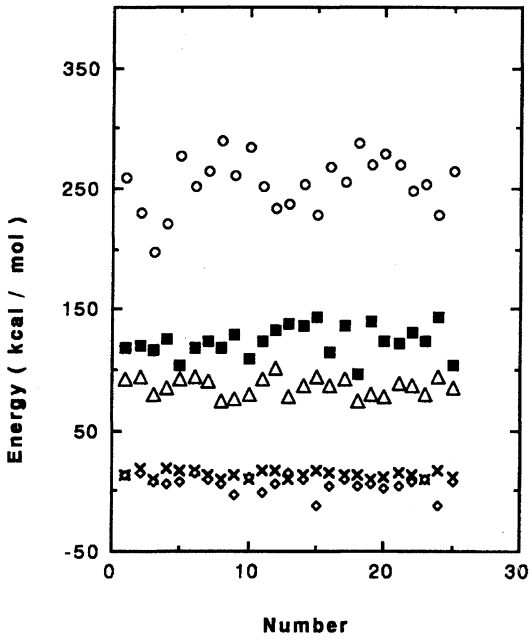

Fig. 7. Energies of the single helical conformers of carradodecaose β-carrageenan after minimization with $\varepsilon=3$. The abscissa indicates the pair number of the dihedral angles. The energy terms are bond (×), angle (△), dihedral (■), van der Walls (◇), and Electrostatics (○), respectively.

energy conformations. However, in this case, there are two other conformers which have similar energy values. One of them is number 18 (d·h helix), whose energy is a little lower than that of number 3 by 1.1 kcal mol^{-1} (dodecamer unit), and the other is the number 8 (b·h

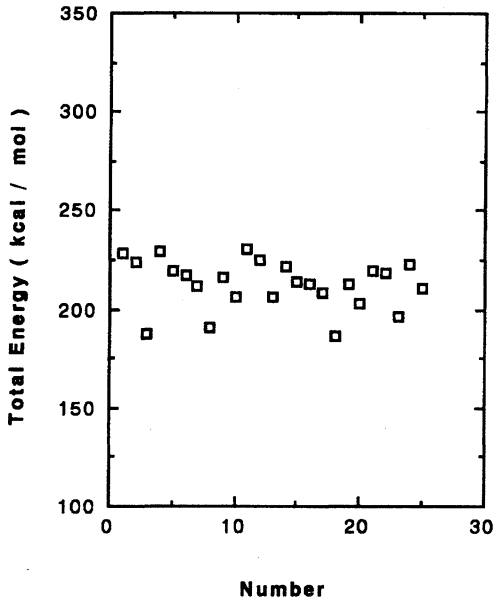

Fig. 8. Total energy of the single helical conformers of carradodecaose β-carrageenan after minimization with $\varepsilon=80$. The abscissa indicates the pair number of the dihedral angles. See the detail in the text.

helix), whose energy is a little higher than that of number 3 by 3.4 kcal mol^{-1} (dodecamer unit). These differences correspond to values of only 0.1 kcal mol^{-1} (1.1 kcal/11 linkages) and 0.31 kcal mol^{-1} (3.4 kcal/11 linkages), respectively, per one glycosidic linkage. These values are sufficiently smaller than the thermal fluctuation energy at room temperature. In this case, the mixed state of these three conformers can be observed at the thermodynamic equilibrium state. That is, the structure of this molecule becomes a coiled conformation. From the above results, it can be said that the single chain of β-carrageenan would exist as a helical conformation, whose dihedral 1–4 linkage angles are in the position of a, and the 1–3 linkage angles are in h, which was obtained from the energy minimization analysis in vacuo with $\varepsilon=3.0$. However, the stability of this structure is not expected to be sufficient, because the extent of the electrostatic shielding by the surrounding solvent molecules strongly affects the conformational stability.

3. Double Helical Conformation. The conformational energy of the double helical structure of β-carrageenan was also examined. In this calculation, the initial coordinates of the double helical structure were built by modification of the data from PDB at Brookhaven National Laboratory,[33] which was obtained by X-ray diffraction experiments of ι-carrageenan of a fiber sample.[34] This initial structure was minimized by the same procedure used in the calculation of the a·h helix, and the energy after the minimization is shown in Table 3. In order to compare this result with those obtained for the single chain structure, values of twice of the energy of the a·h helix structure, which corresponds to the energy of the chain with 12×2 residues, are shown in parentheses. In the calculation of $\varepsilon=3$, the total energy of the double helix structure was found to be a little higher than that of the a·h helix by 12.8 kcal mol^{-1}, when the comparison was made for the same 12×2 residues. This energy difference corresponds to a values of 0.5 kcal mol^{-1} per monosaccharide unit. This small energy difference indicates that the double helical structure is as stable as that of the a·h helix. Comparison of each energy term between the a·h single helix and the double helix shown in Table 3 shows the difference of the stabilization factor for these structures. In the van der Waals forces term, the energy value of the double helix is considerably lower than that of the a·h helices (×2) by about 63 kcal mol^{-1}. On the contrary, the energy of the electrostatic force of the double helix is 50 kcal mol^{-1} higher than that of the a·h helices (×2). In terms of such short range interactions as bond, angle, and dihedral interactions, there are no large differences in the energy values. This indicates that the stability of the double helix comes mainly from van der Waals forces, even though the electrostatic force plays an important role in the stabilization of the a·h helix as was discussed in the previous section. For this reason, the double helical structure may be expected to exist as a stable form even in an environment where the electrostatic force is strongly shielded. Actually, the results calculated with $\varepsilon=80$, where the electrostatic interaction might be expected to become less important, indicate that the relative stability of the double helical structure is effectively increased in comparison to that of the a·h helix by about 33 kcal mol^{-1} in total energy. This indicates that the double helical structure may be little affected by the surrounding solvent molecules because its stabilization factor is van der Waals forces.

To investigate the stability of the double helical structure further, the energy of an isolated single helical strand with the same geometry as the double helix was calculated and compared with those of the parent double helix. The calculated values are also shown in Table 3. It can be seen that this strand is very unstable. The electrostatic force energy of this strand is 108 kcal mol^{-1} higher than that of the parent double helix, when the comparison was made on the same 12×2 residues. The energy of the van der Waals forces is also 46 kcal mol^{-1} higher, although the short range energy terms, such as bond, angle, and dihedral energies are almost the same. These energy differences in the long range terms clearly correspond to the interaction energy between the two chains of the double helix. The above results clearly indicate that the formation of the double helical structure from two corresponding single chains can effectively lower the energy of the long rang terms by strong interactions between the helical strands of the double helix. The instability of this single helical strand was also clearly shown by comparison with the a·h single helix, because the total energy is 78 kcal mol^{-1} higher than that of the a·h helix in the calculation of $\varepsilon=3$. The values of the glycosidic torsion angles of this single helical strand correspond to those of a b·h helix, which is one of the single helical conformers discussed in the previous section (number 8 in Figs. 4 and 8). The calculation with a dielectric constant $\varepsilon=80$ also indicates the instability of this helix compared to the double helical conformation, but its energy was considerably lowered and almost similar to the value of the a·h helix. This situation is clearly shown in Fig. 8, because the energy of a single strand corresponds to that of number 8 in this figure. However, this conformation is, of course, unstable as discussed previously.

4. Molecular Dynamics. In the above molecular mechanics treatments, the molecule is settled at the minimum energy position at 0 K. In a real solution, the molecule dynamically fluctuates its energy at room temperature. In order to investigate the stability of the molecules under such conditions, the time course of the molecular motion under thermal fluctuation must be analyzed. Therefore, molecular dynamics simulations of the above three models of the helical structure were performed at 300 K. Figure 5 shows both stereo views of the minimum energy conformation of the a·h helix

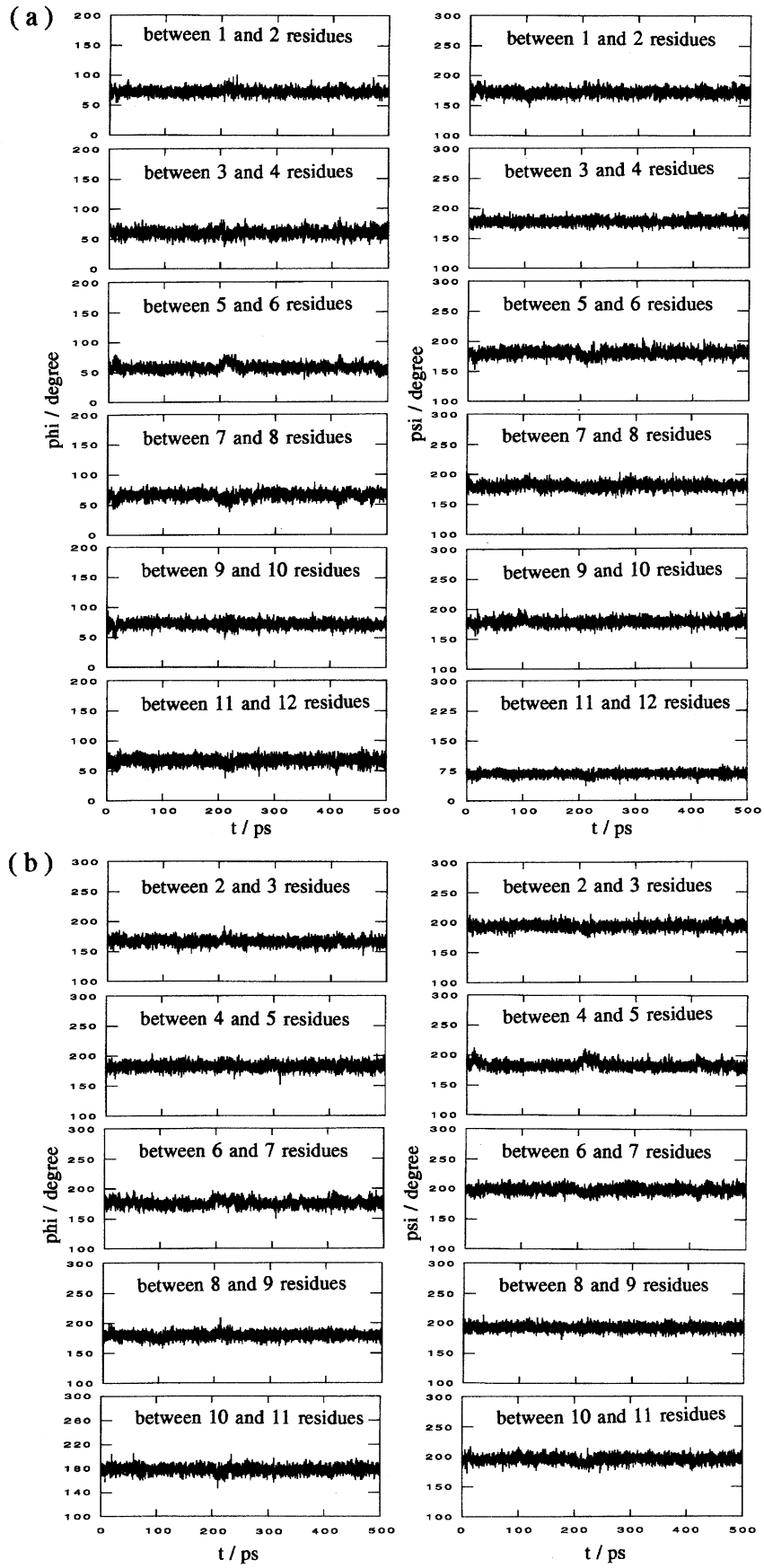

Fig. 9. History of all dihedral angles ϕ and ψ between the 1—4 linked **B–A** residues (a), and between the 1–3 linked **A–B** residues (b) of the single helical conformation of β-carrageenan with a·h pair dihedrals. The calculations were done with $\varepsilon=3$.

Table 3. Comparison of the Energies between Single and Double Helical Conformations after Minimization

		Number of residues	Energy/kcal mol^{-1}					
			Total	Bond	Angle	Dihedral	VDW	Electric
	a·h-Helix	12	413.0	10.1	80.9	117.1	8.1	196.8
	(×2)	(12×2)	(826.0)	(20.2)	(161.8)	(234.2)	(16.2)	(393.6)
ε=3	Double-helix	12×2	838.8	18.2	161	262.2	−46.6	443.9
	Single-strand of double helix	12	490.7	11.8	76.1	127.4	−0.5	275.8
	(×2)	(12×2)	(981.4)	(23.6)	(152.2)	(254.8)	(−1.0)	(551.6)
	a·h-Helix	12	187.6	7.2	74.7	107.2	−13.6	12.1
	(×2)	(12×2)	(375.2)	(14.4)	(149.4)	(214.4)	(−27.2)	(24.2)
ε=80	Double-helix	12×2	341.8	11.7	144.6	216.5	−57.9	26.9
	Single-strand of double helix	12	191.6	6.3	71.3	96.4	4.2	13.5
	(×2)	(12×2)	(383.2)	(12.6)	(142.6)	(192.8)	(8.4)	(27.0)

after the minimization, which was used as an initial structure of the dynamics calculation(a), and a snap shot at the 500 ps dynamics after a 50 ps equilibration run(b). It can be seen that the helical structure remains stable after the 500 ps dynamics run. In order to analyze the stability of the helix more quantitatively, the time courses of the dihedral angles (ϕ,ψ) of all glycosidic linkages between the **B–A** and **A–B** residues of the a·h helix are shown in Fig. 9. All dihedral angles remain in their initial positions in all time courses observed, that is, the dihedral angles of (ϕ,ψ) between the **B** and **A** residues are fluctuating around position a (ϕ=67°, ψ=173°) and those between the **A** and **B** residues are around position h (ϕ=175°, ψ=182°). This indicates that the a·h helical structure keeps its structure during the time course examined. In order to survey the stability of the whole structure of this helix, the time course of the distance between two arbitrarily selected glycosyl oxygen atoms was investigated. Figure 10 shows the time course of the distance between two glycosyl oxygen atoms, one was selected from the linkage between the A2 and B3 residues and the other from that between the A10 and B11 residues. Except for the spontaneous large fluctuation at 200 ps, the distance stays at a mean value of 8.4 Å with a simple oscillation around it. This also indicates that the a·h helix keeps its structure during the time courses examined.

Similar dynamic calculations were performed on the same a·h single helix by using ε=80. The time courses of the dihedral angles (ϕ,ψ) of all glycosidic linkages between the **B–A** and **A–B** residues are shown in Fig. 11. Although the initial values of these dihedral angles were all set at the a·h position, the angles between the B11–A12 residues were changed from position a to values around the ϕ=170° and ψ=180° (position b) as was shown in Fig. 11(b). This indicates that the position a is no longer unique stable position in the condition of ε=80 as was discussed in the section on energy minimization. However, the transitional behavior between the wells of a and b, and/or b and d can not be observed in the period of this dynamics run. This is partly because the potential barriers between a and b and/or b and d are too high (6—8 kcal mol^{-1}) compared to the energy of the thermal fluctuation at room temperature as was shown in Fig. 3, and therefore, more long time simulation may be needed to simulate the interchange behavior of the dihedral angles of the glycosidic linkages. As for the behavior of the dihedral angles of the 1–3 linked **A–B** residues (Fig. 11(a)), large fluctuations in ψ were found. This fluctuation corresponds to the movement from h to i in Fig. 3. The increment of the shielding effect of the electrostatic field increases the fluctuation of this molecule.

Molecular dynamics calculations were also performed on the carradodecaose double helix of β-carrageenan. In this case, the dynamics of 250 ps after the 50 ps equilibration were simulated. Figure 12 shows stereo views of the initial structure of the double helical conformation after energy minimization(a) and its snapshot after the 300 ps dynamics run(b). The double helical structure

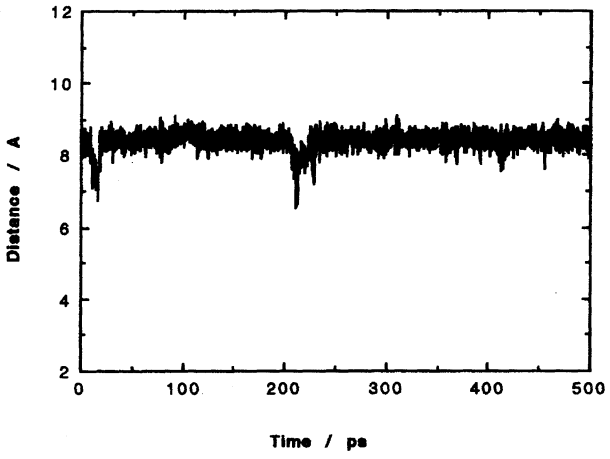

Fig. 10. History of the distance between the glycosidic oxygens between the residues of A2–B3 and the A10–B11 of the single helical conformation of β-carrageenan with a·h pair dihedrals.

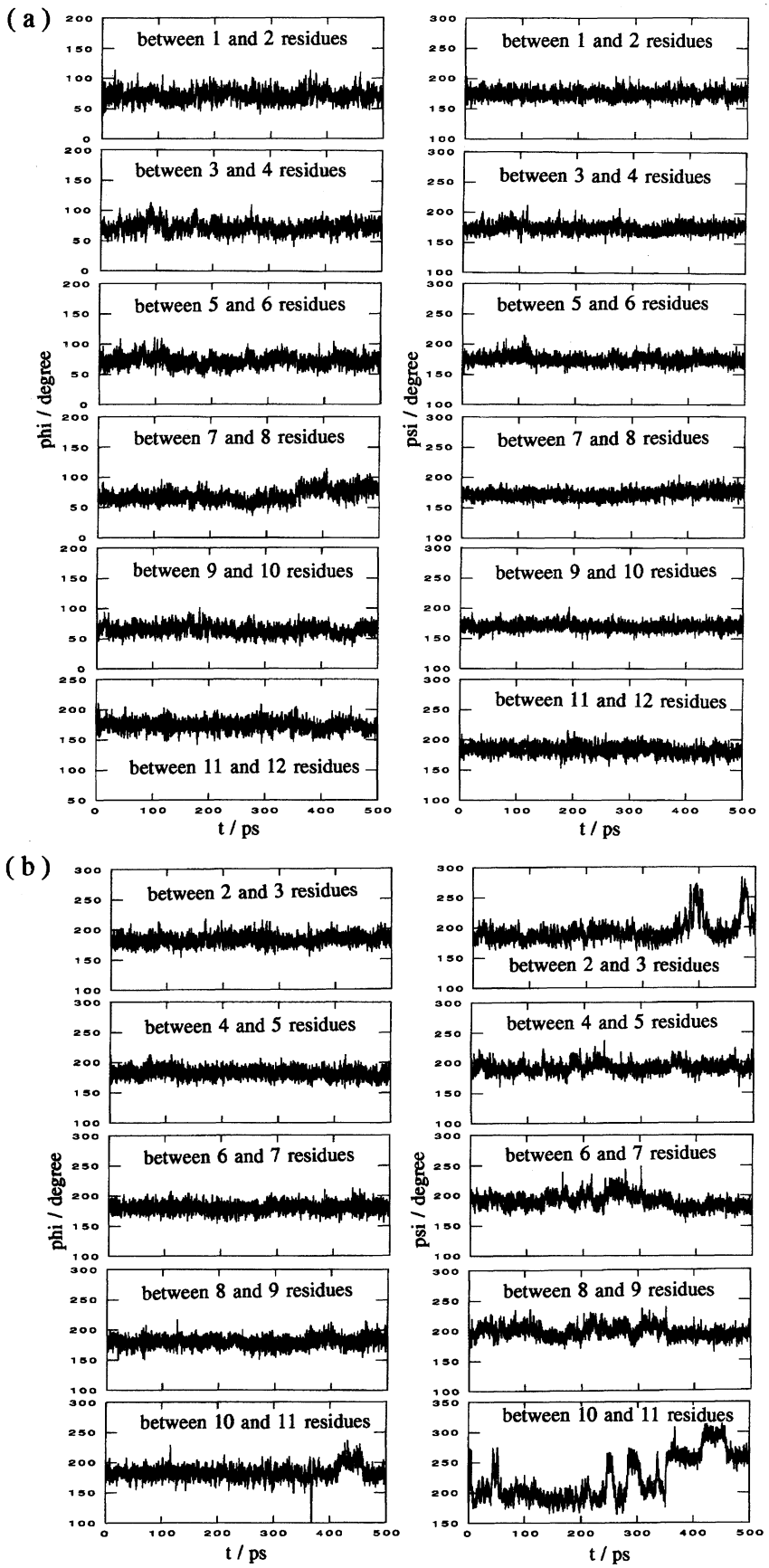

Fig. 11. History of all dihedral angles ϕ and ψ of the 1—4 linked **B–A** residues (a), and the 1–3 linked **A–B** residues (b) of the single helical conformation of β-carrageenan with a·h pair dihedrals. The calculations were done with ε=80.

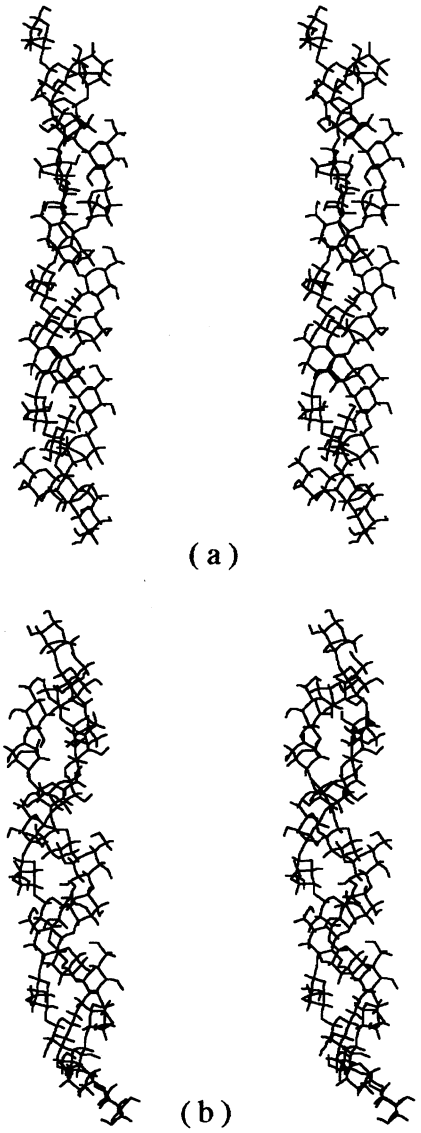

Fig. 12. Stereo views of the initial conformation after minimization and its snapshot at the 300 ps dynamics of the double helix conformation of β-carrageenan with carradodecaose chains.

is sustained also in this case. The molecular motion of the whole time course was monitored by video animation. The double helical structure was dynamically oscillated, but no large bends or kinks along the helical axis were observed. The distance between the glycosyl oxygen atoms between the same residues denoted on the a·h helix was also monitored in the period of 250 ps after the 50 ps equilibration (Fig. 13). The average value of the distance was 32.5 Å which did not change during the time courses. In addition, the calculated value of the deviation from the mean value is ±0.13 Å. This value is smaller than that of the a·h helix (±0.19 Å). This may indicate that the double helical structure is more rigid than the a·h helix. The molecular dynamics of the isolated single helical strand with the same geometry as the double helix were also investi-

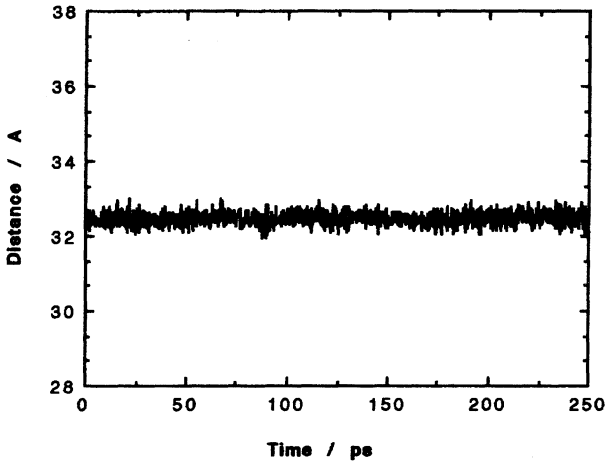

Fig. 13. History of the distance between the glycosidic oxygens between the residues of A2–B3 and the A10–B11 of the double helical conformation of β-carrageenan

gated. The initial structure after energy minimization-(a) and the snapshot of the 500 ps dynamics run after the 50 ps equilibration(b) are shown in Fig. 14. The elongated helical structure at the initial stage changed its conformation dynamically and formed another helical structure with a large loop. From a snapshot after the 550 ps dynamics in Fig. 14, the helical structure was found to have a loop of 8 residues per turn. This loop structure is basically the same as that of the a·h helix. Although the helical pitch along to the axis is different, this structure may approach the a·h helix after long time dynamics. The trace of the distance between the glycosyl oxygen as defined above is shown in Fig. 15. The distance shows an abrupt decrease at about 200 ps in the analysis run. The fluctuation is also large compared to those of other helices as shown in Figs. 10 and 13. These results clearly confirm the instability of this single helical structure.

Conclusion

As a first step in the computer simulation investigation of the solution conformation of the carrageenan family, the conformation of β-carrageenan in vacuo was analyzed by molecular mechanics and molecular dynamics calculations. The results were as follows. A possible structure of the single helical form of β-carrageenan was elucidated whose helix has a large loop with 8 residues per turn. The obtained structure is similar to the well-known ring structure of γ-cyclodextrin with the same 8 sugar residues in its ring structure. By analogy with the properties of cyclodextrin, β-carrageenan may be able to form a host–guest inclusion compound. The stability of this helical form, however, was found to depend strongly on the shielding effect of the electrostatic field of the surrounding solvent molecules. In the simulation with strong shielding by the electrostatic force, this single helix was found to be no more stable, and may be a

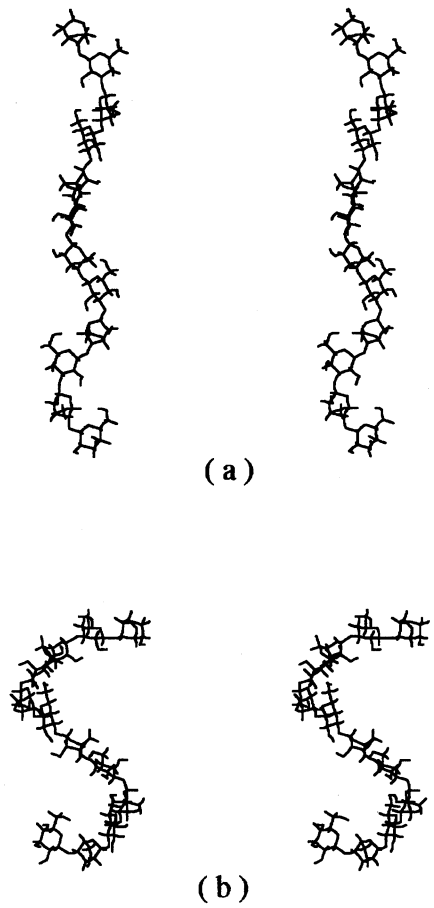

Fig. 14. Stereo views of the initial conformation after minimization and its snapshot at the 550 ps dynamics of the single helical strand part of the double helical β-carrageenan.

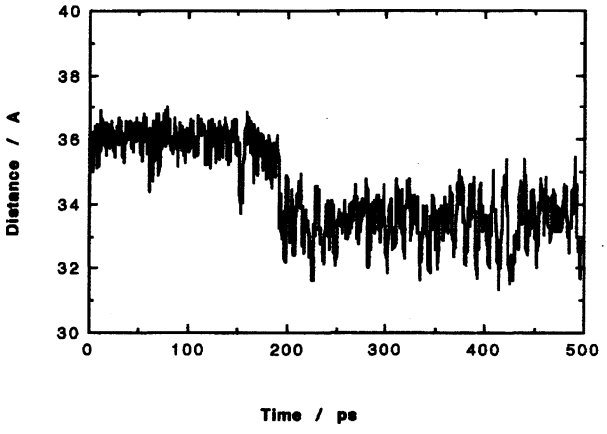

Fig. 15. History of the distance between the glycosidic oxygens between the residues of A2–B3 and the A10–B11 of the single strand part of the double helical β-carrageenan.

random coiled conformation.

The structure of the double helical conformation obtained from X-ray diffraction was found to have roughly equal stability to the a·h type single helix from the potential energy analysis. This conformation is mainly stabilized by van der Waals forces, not the electrostatic forces. For this reason, the structure was still stable in the calculation of $\varepsilon=80$. This may indicate that the double helical conformation would exist more stably than the single helical structure, because the single helical conformation depends strongly on the electrostatic environment of the surrounding molecules. In this study, the effect of the solvent molecules was limited by the dielectric constant in these conditions that they merely work as a shielding medium of the electrostatic forces. However, other important roles of the solvent molecules in polysaccharide conformation are solvation and hydrogen bonding between the solute–solvent molecules. Brady and Schmidt[10] revealed that a wide variety of hydrogen bonds are formed in carbohydrate solutions. For an estimation of this effect, the solvent molecules should be included explicitly in the calculation. A study in this direction will be discussed as the next step using the model structures found in this work. Comparative studies between the conformation of β-carrageenan found in this study and the κ- and ι-carrageenan with sulfate groups will also be done in the near future.

The authors thank Daicel Chemical Co., Ltd. for financial support.

References

1) A. A. McKinnon, D. A. Rees, and F. B. Williamson, *J. Chem. Soc., Chem. Commun.*, **1969**, 701.
2) D. A. Rees, *Biochem. J.*, **126**, 257 (1972).
3) E. R. Morris, D. A. Rees, and G. Robinson, *J. Mol. Biol.*, **138**, 349 (1980).
4) N. S. Anderson, J. W. Campbell, M. M. Harding, D. A. Rees, and J. W. B. Samuel, *J. Mol. Biol.*, **45**, 85 (1969).
5) O. Smidsrod and H. Grasdalen, *Carbohydr. Polym.*, **2**, 270 (1982).
6) C. Rochas and M. Rinaudo, *Biopolymers*, **23**, 735 (1984).
7) T. A. Bryce, A. H. Clark, D. A. Rees, and D. S. Reid, *Eur. J. Biochem.*, **122**, 63 (1982).
8) S. Paoletti, O. Smidsrod, and H. Grasdalen, *Biopolymers*, **23**, 1771 (1984).
9) A. M. Hermansson, "Physical Networks, Polymers and Gels," ed by W. Burchard and S. B. Ross-Murphy, Elsevier, London (1990), p. 271.
10) J. W. Brady and R. K. Schmidt, *J. Phys. Chem.*, **97**, 958 (1993).
11) "Computer Modeling of Carbohydrated Molecules," ed by A. D. French and J. W. Brady, ACS Symposium Series 430, American Chemical Society, Washington, D. C. (1990).
12) S. W. Homans, *Biochemistry*, **29**, 9110 (1990).
13) B. J. Hardy and A. Sarko, *J. Comput. Chem.*, **14**, 848 (1993).
14) B. J. Hardy and A. Sarko, *J. Comput. Chem.*, **14**, 831 (1993).
15) M. K. Dowd, P. J. Reilly, and A. D. French, *J. Com-*

put. Chem., **13**, 102 (1992).
16) G. A. Jeffery and R. Taylor, *J. Comput. Chem.*, **1**, 99 (1980).
17) W. Zhang, L. Piculell, and S. Nilsson, *Biopolymers*, **31**, 1727 (1991).
18) B. R. Brooks, R. E. Bruccoleri, B. D. Olafson, D. J. States, S. Swaminathan, and M. Karpulus, *J. Comput. Chem.*, **4**, 187 (1983).
19) S. N. Ha, A. Giammono, M. Field, and J. W. Brady, *Carbohydr. Res.*, **180**, 207 (1988).
20) J. W. Brady, *J. Am. Chem. Soc.*, **108**, 8153 (1986).
21) I. Tvaroska, C. Rochas, F. R. Travel, and T. Turquois, *Biopolymers*, **32**, 551 (1992).
22) M. Dauchez, P. Derreumaux, and G. Vergoten, *J. Comput. Chem.*, **14**, 263 (1992).
23) "Gaussian 92, Revision C. 4," ed by M. J. Frisch, G. W. Trucks, M. Head-Gordon, P. M. W. Gill, M. W. Wong, J. B. Foesman, B. G. Johnson, H. B. Schlegel, M. A. Robb, E. S. Replogle, R. Gomperts, J. L. Andres, K. Raghavachari, J. S. Binkley, C. Gonzalez, R. L. Martin, D. J. Fox, D. J. Defrees, J. Baker, J. J. P. Stewart, and J. A. Pople, Gaussian Inc., Pittsburgh, PA (1992).
24) K. Ueda, H. Ochiai, A. Imamura, and S. Nakagawa, *Koubunshi Ronbunshu*, **94**, 400 (1994).
25) B. H. Besler, K. M. Merz, Jr., and P. A. Kollman, *J. Comput. Chem.*, **11**, 431 (1990).
26) U. C. Singh and P. A. Kollman, *J. Comput. Chem.*, **5**, 129 (1984).
27) M. L. Bender and M. Komiyama, "Cyclodextrin Chemistry," Springer-Verlag, Berlin (1978).
28) "Starch and Its Components," ed by W. Banks and C. T. Greenwood, Edinburgh University Press, Edinburgh (1975).
29) A. Sarko and H. -C. H. Wo, *Starch*, **30**, 73 (1978).
30) W. Schultz, H. Sklenar, W. Hinrichs, and W. Saenger, *Biopolymers*, **33**, 363 (1993).
31) K. Okuyama, A. Otubo, Y. Fukazawa, M. Ozawa, T. Harada, and N. Kasai, *J. Carbohydr. Chem.*, **10**, 645 (1991).
32) Y. Deslandes, R. T. Marchessault, and A. Sarko, *Macromolecules*, **13**, 1466 (1980).
33) F. C. Bernstein, T. F. Koetzle, G. J. B. Williams, E. F. Meyer, Jr., M. D. Brice, J. R. Rodgers, O. Kennard, T. Shimanouchi, and M. Tasumi, *J. Mol. Biol.*, **112**, 535 (1977).
34) S. Arnott, W. E. Scott, D. A. Rees, and C. G. A. McNab, *J. Mol. Biol.*, **90**, 253 (1974).